

Application of a Langmuir probe AC technique

Application of a Langmuir probe AC technique for reliable access to the low energy range of electron energy distribution functions in low pressure plasmas

A. Heiler,^{1, 2, a)} R. Friedl,² and U. Fantz^{1, 2}

¹⁾*Max-Planck-Institut für Plasmaphysik, Boltzmannstrasse 2, D-85748 Garching, Germany*

²⁾*AG Experimentelle Plasmaphysik, Universität Augsburg, D-86135 Augsburg, Germany*

(Dated: 6 February 2020)

The electron energy distribution function (EEDF) in low pressure plasmas is typically evaluated by using the second derivative d^2I/dV^2 of a Langmuir probe I - V characteristic (Druyvesteyn formula). Since measured probe characteristics are inherently noisy, two-time numerical differentiation requires data smoothing techniques. This leads to a dependence on the employed filtering technique and information particularly in the region near the plasma potential can easily get lost. As an alternative to numerical differentiation of noisy probe data, a well-known AC probe technique is adopted to measure d^2I/dV^2 directly. This is done by superimposing a sinusoidal AC voltage of 13 kHz on the probe DC bias and performing a Fourier analysis of the current response. Parameters like the modulation amplitude (up to 1.5 V) and number of applied sine oscillations per voltage step of the DC ramp are carefully chosen by systematic parameter variations. The AC system is successfully benchmarked in argon and applied to hydrogen plasmas at a laboratory ICP experiment (4 – 10 Pa gas pressure, 300 – 1000 W RF power). It is shown that the EEDF is reliably accessible with high accuracy and stability in the low energy range. Hence, a trustworthy determination of basic plasma parameters by integration of the EEDF can be provided.

^{a)}Electronic mail: adrian.heiler@ipp.mpg.de

Application of a Langmuir probe AC technique

I. INTRODUCTION

The kinetic energy distribution of electrons in low pressure plasmas is a crucial parameter because it is the main determinant for the rate of occurring reactions like ionization, dissociation or excitation processes. Since it is known that the electron ensemble is often not in thermal equilibrium^{1,2}, the electron energy distribution function (EEDF) can deviate significantly from a Maxwellian shape. Hence, an accurate determination of the EEDF is indispensable for a proper evaluation of basic plasma parameters, rates of plasma-chemical processes or modeling approaches. To determine the EEDF experimentally in terms of number of electrons per kinetic energy interval $[\epsilon_e, \epsilon_e + d\epsilon_e]$ and unit volume, a Langmuir probe current-voltage (I - V) characteristic is usually used and the well-known Druyvesteyn formula is applied. This formula correlates the EEDF with the second derivative of the electron current I_e drawn by the probe in the retarding potential region, i. e. for applied voltages below the plasma potential ϕ_{pl} ³:

$$\text{EEDF}(\epsilon_e) = \frac{\sqrt{8m_e}}{e^3 A_p} \sqrt{\epsilon_e} \frac{\partial^2 I_e}{\partial V^2}, \quad (1)$$

with the electron energy $\epsilon_e = e(\phi_{pl} - V)$, the probe electrode area A_p , the electron mass m_e and the elementary charge e . The Druyvesteyn formula is valid for any convex probe geometry⁴ under the assumption of an isotropic electron velocity distribution with no time variation and spatial gradient. However, it can only be applied in the collisionless probe regime, meaning that the charged particles do not collide in the probe sheath and can reach the probe conserving their energies and momenta. Moreover, it has to be taken into account that the measured probe current I_p consists of both negatively and positively charged particles. As discussed in Ref. 5 though, $\partial^2 I_e / \partial V^2 \approx \partial^2 I_p / \partial V^2$ is usually a good approximation for the noise-limited dynamic range of the EEDF in most measurements.

The most straightforward and commonly used technique to determine the second derivative is two-time numerical differentiation of the I - V characteristic. However, using this approach, special attention must be paid to the accuracy of the measured probe curve since even small perturbations or fluctuations can lead to enormous distortions in the second derivative due to error magnification^{6,7}. As described in detail by Godyak and Demidov⁵, especially the low energy range of the EEDF is highly sensitive to the differentiation procedure because the second derivative falls from its maximum to zero when reaching the plasma potential. This sharp drop is a challenging task to measure and requires sophisticated probe systems and evaluation techniques

Application of a Langmuir probe AC technique

due to the following reasons. First of all, measured probe data are inherently noisy and therefore the application of some noise suppression method is indispensable for the differentiation process. Dependent on the noise level, chosen filtering technique (e. g. Savitzky-Golay, Gaussian or Blackman filter) and the applied filter parameters, this can lead to a severe distortion of the maximum of the second derivative and a widening of the interval between the maximum and zero of several volts^{6,8,9}. Furthermore, the voltage drop across various resistances in the probe circuit can affect the I - V characteristic particularly near the plasma potential where the probe current is high and the probe-sheath resistance is low. Without consideration of these stray voltages, which are often hardly quantifiable, the applied voltage to the probe can be overestimated and double differentiation of an even slightly distorted I - V characteristic can lead again to a flattening effect near the plasma potential^{5,8}. In radio frequency (RF) discharges interfering RF voltages in the probe sheath may lead to additional distortions caused by the measurement of time-averaged probe currents¹. Thus, various RF compensation techniques with active or passive filter designs have been developed over the last decades. In practice, however, it is often extremely difficult to achieve sufficient RF compensation for various plasma conditions¹⁰ and it has been shown that already small RF distortions can lead to highly erroneous EEDFs especially near zero electron energy¹¹⁻¹³.

As an alternative to numerical differentiation several different approaches have been developed over the last decades to determine the second derivative of an I - V curve. Common methods are differentiation circuits, where the derivative is measured in the time domain with the use of operational amplifiers^{11,14-16}, and AC modulation techniques, which are based on the filtering of some imposed frequency components in the probe current¹⁷⁻²⁵. Moreover, Jauberteau and Jauberteau²⁶ applied an AC superimposition method numerically in order to determine derivatives of a noisy function and Bang and Chung²⁷ demonstrated its noise suppression efficiency for measured EEDFs especially in the high energy region. In this work, a newly developed Langmuir probe system is presented that incorporates a sine wave modulation of the output voltage applied to the probe, which was first proposed by Sloane and MacGregor²⁸ and has the advantage of a rather simple circuit design. The AC system is implemented at an inductively coupled plasma (ICP) experiment and a reliable access to the EEDF low energy range is demonstrated in argon and hydrogen. By comparison to a conventional DC probe system using numerical differentiation with Savitzky-Golay (SG) smoothing²⁹, it is shown that the AC result is more robust against small fluctuations and errors in the probe current especially near zero energy.

Application of a Langmuir probe AC technique

II. LANGMUIR PROBE AC METHOD

A. Sheath generated harmonics and second derivative

The AC method used in this work exploits the generation of harmonics in the probe current by applying a sinusoidal AC voltage²⁸. This effect is illustrated in Fig. 1 for an exemplary I - V curve. The applied modulated voltage to the probe

$$\tilde{V}(t) := V + v(t) = V + v_0 \sin(2\pi vt) \quad (2)$$

with DC bias V , sine amplitude v_0 and frequency v leads to a non-sinusoidal current response due to the nonlinear sheath impedance and can be expressed by a Taylor series as

$$\begin{aligned} I_p(\tilde{V}) &= \sum_{n=0}^{\infty} \frac{I_p^{(n)}(V)}{n!} v^n \\ &= I_p(V) + v I_p'(V) + \frac{v^2}{2} I_p''(V) + \frac{v^3}{6} I_p'''(V) + \dots \end{aligned} \quad (3)$$

with $I_p' \equiv \partial I_p / \partial V$, $I_p'' \equiv \partial^2 I_p / \partial V^2$ etc. From this, it can be shown that the frequency component I_p^{2v} associated with the second harmonic of the modulation frequency has contributions only from even-order derivatives and is given by²⁶

$$\begin{aligned} I_p^{2v}(V) &= \sum_{n=1}^{\infty} \frac{v_0^{2n} \cdot I_p^{(2n)}(V)}{2^{2n-1} \Gamma(n) \Gamma(n+2)} \\ &= \frac{v_0^2}{4} I_p''(V) + \frac{v_0^4}{48} I_p^{(4)}(V) + \frac{v_0^6}{1536} I_p^{(6)}(V) + \dots \end{aligned} \quad (4)$$

with the Gamma function Γ . Neglecting the terms involving the fourth and higher order derivatives, the second derivative of the probe current can thus be approximated by

$$I_{p,AC}''(V) = \frac{4}{v_0^2} I_p^{2v}(V). \quad (5)$$

Hence, Fourier transformation of the AC perturbed probe current for $\tilde{V} \leq \phi_{pl}$ directly determines the EEDF by using the Druyvesteyn formula:

$$\text{EEDF}(\epsilon_e) = \frac{\sqrt{8m_e}}{e^3 A_p} \sqrt{\epsilon_e} \frac{4}{v_0^2} I_p^{2v}(\phi_{pl} - V). \quad (6)$$

Application of a Langmuir probe AC technique

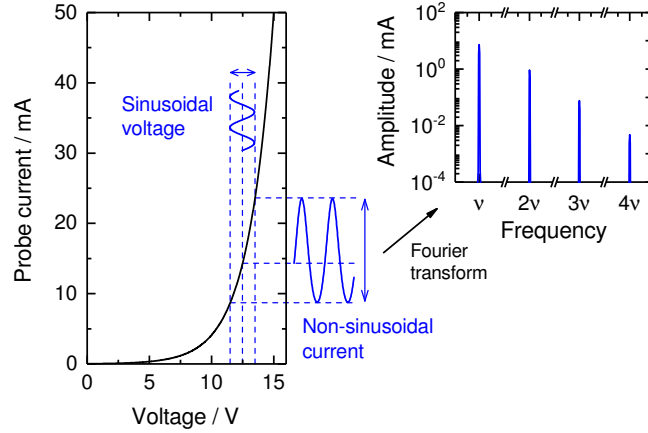


FIG. 1. Illustration of the Langmuir probe AC method: an applied sinusoidal voltage with frequency ν leads to a non-sinusoidal probe current caused by the nonlinear sheath impedance. The frequency spectrum shows that the modulated probe current consists of integer multiples of ν .

B. Systematic error of AC second derivative

The neglect of the fourth and higher order derivatives in Eq. (4) leads to an overestimation of the determined second derivative via Eq. (5). In order to study this systematic error in more detail, the DC electron current for a Maxwellian EEDF is used:

$$I_e(V \leq \phi_{pl}) = I_e(\phi_{pl}) \exp \left[\frac{e(V - \phi_{pl})}{k_B T_e} \right], \quad (7)$$

where $I_e(\phi_{pl}) = eA_p n_e \sqrt{k_B T_e / (2\pi m_e)}$, n_e denoting the electron density, T_e the electron temperature and k_B the Boltzmann constant³⁰. The analytical second derivative of Eq. (7) is given by

$$I_e''(V) = \frac{e^2}{(k_B T_e)^2} I_e(V). \quad (8)$$

Using expression (7) to simulate the AC perturbed probe current yields

$$\begin{aligned} I_e[\tilde{V}(t)] &= I_e(V) \exp[x_0 \sin(2\pi\nu t)] \\ &= I_e(V) \left[I_0(x_0) + 2 \sum_{j=1}^{\infty} I_j(x_0) \sin(2\pi j\nu t) \right] \end{aligned} \quad (9)$$

with $x_0 = e\nu_0 / (k_B T_e)$ and the modified Bessel functions of the first kind I_j with integer order j ³¹. As can be seen easily, the current amplitude at twice the modulation frequency can be written as

$$I_e^{2\nu}(V) = I_e(V) 2I_2(x_0) \quad (10)$$

Application of a Langmuir probe AC technique

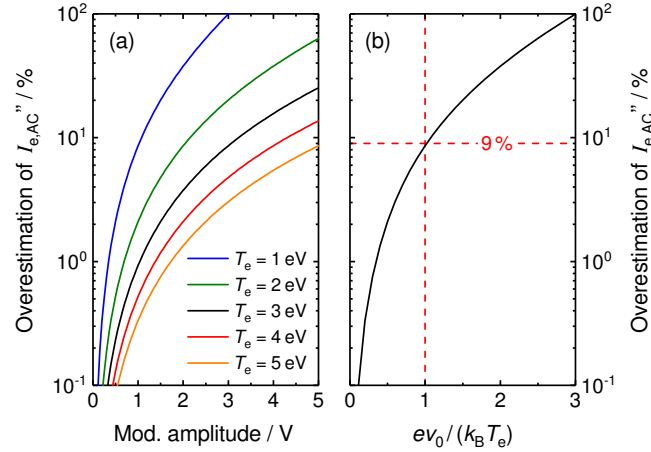


FIG. 2. Simulated overestimation of the second derivative determined via the AC technique for Maxwellian electron currents (a) as a function of modulation amplitude for varying electron temperatures and (b) depending on the ratio of modulation amplitude to electron temperature.

and the simulated second derivative is given by

$$I''_{e,AC}(V) = \frac{8}{v_0^2} I_e(V) I_2(x_0). \quad (11)$$

From this, the relative overestimation of the AC second derivative compared to the analytical value (8) is

$$\xi(x_0) = \frac{I''_{e,AC} - I''_e}{I''_e} = 8x_0^{-2} I_2(x_0) - 1 \quad (12)$$

and depends both on the modulation amplitude and the temperature of the plasma electrons. In Fig. 2(a) ξ is plotted as a function of v_0 up to 5 V for electron temperatures in the range of 1 – 5 eV. Increasing the modulation amplitude and decreasing the electron temperature lead to a higher error in the determined second derivative, caused by an increasing ratio of the neglected terms to the first term in Eq. (4). As can be seen in Fig. 2(b), this overestimation stays below 9 % for $x_0 \leq 1$.

C. Influence of distortion frequencies

If distortion frequencies couple into the experiment and hence to the probe sheath, an additional error emerges caused by intermodulation with the applied modulation frequency. In case of only one distortion frequency ν_{dis} with amplitude ν_{dis} and phase angle ϕ_{dis} , the respective Taylor

Application of a Langmuir probe AC technique

expansion leads to the following modification of Eq. (4):

$$I_p^{2\nu}(V) = \frac{v_0^2}{4} I_p''(V) + \left(\frac{v_0^4}{48} + \frac{v_0^2 v_{\text{dis}}^2}{16} \right) I_p^{(4)}(V) + \left(\frac{v_0^6}{1536} + \frac{v_0^4 v_{\text{dis}}^2}{192} + \frac{v_0^2 v_{\text{dis}}^4}{256} \right) I_p^{(6)}(V) + \dots \quad (13)$$

This approximation is valid under the assumption that no intermodulation products occur at twice the modulation frequency, i. e. $a\nu + b\nu_{\text{dis}} \neq 2\nu$ with $a, b \in \mathbb{Z}$. The additional contributions in Eq. (13) compared to Eq. (4) lead to an increased overestimation of $I_{e,\text{AC}}''$. In the Maxwellian case, the probe current given in Eq. (9) now has to be multiplied by

$$I_0(x_{\text{dis}}) + 2 \sum_{j=1}^{\infty} I_j(x_{\text{dis}}) \sin(2\pi j\nu_{\text{dis}}t + \varphi_{\text{dis}}) \quad (14)$$

with $x_{\text{dis}} = e\nu_{\text{dis}}/(k_{\text{B}}T_e)$ and the frequency independent DC current term $I_0(x_{\text{dis}})$ gives an additional contribution to the second harmonic $I_e^{2\nu}$. This leads to

$$I_{e,\text{AC}}''(V) = \frac{8}{v_0^2} I_e(V) I_2(x_0) I_0(x_{\text{dis}}) \quad (15)$$

and

$$\xi(x_0, x_{\text{dis}}) = 8x_0^{-2} I_2(x_0) I_0(x_{\text{dis}}) - 1. \quad (16)$$

In Fig. 3(a) the dependence of ξ on the modulation and distortion amplitude is demonstrated up to 5 V for $T_e = 3$ eV. In analogy to Fig. 2(b), the contour line of $\xi(x_0, x_{\text{dis}}) = 9\%$ is highlighted in Fig. 3(b).

D. Application in experiment

For the experimental application of the AC method in this work, the probe current signal is digitized via a data acquisition system using a certain sampling frequency. Therefore, the influence of additional oscillations in the probe sheath would not only be dependent on their amplitudes, but also on their frequencies, phase shifts and the sampling rate used. If, for instance, a voltage oscillation with a higher frequency than the sampling frequency is present, many cycles lie in between one sample and the next, and the current-voltage correlation is dependent on when the sample is taken. Hence, for the experimental application of the AC technique it is necessary to analyze first the voltage oscillations across the probe sheath considering two aspects: on the one hand, the modulation frequency and its harmonics must not be superimposed and on the other

Application of a Langmuir probe AC technique

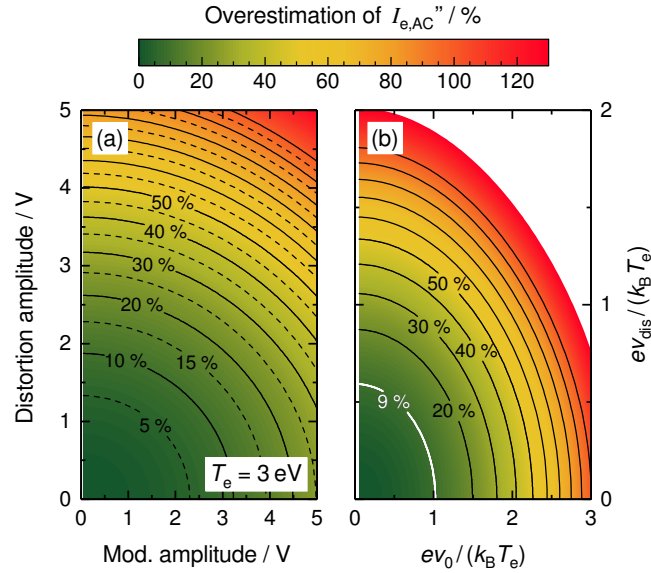


FIG. 3. Simulated overestimation of the second derivative determined via the AC technique for a Maxwellian EEDF with adding a distortion frequency, as a function of (a) modulation and distortion amplitude for $T_e = 3$ eV and (b) ratio of modulation and distortion amplitude to the electron temperature.

hand, the distortion amplitudes over the whole frequency range have to be small compared to the modulation amplitude. This is especially important for situations where the plasma potential is fluctuating. Consequently, a compensated Langmuir probe should be used in an RF plasma where frequencies usually in the MHz range are present.

In general, the modulation frequency should lie far below the electron plasma frequency. Moreover, it should be noted that the modulation frequency has to be sufficiently low so that displacement currents

$$I_{\text{disp}}(t) = \frac{d}{dt} [C_{\text{sh}}(t)v(t)] \quad (17)$$

with the probe sheath capacitance C_{sh} can be neglected. Since the sheath capacitance depends on the voltage difference between the plasma and the probe potential³², it changes in response to the applied voltage oscillations and has thus a time dependence. For typical values of $v_0 \sim 1$ V and $C_{\text{sh}} \sim 1$ pF the modulation frequency has to be $\lesssim 100$ kHz in order to keep the displacement current below 10^{-6} A.

Application of a Langmuir probe AC technique

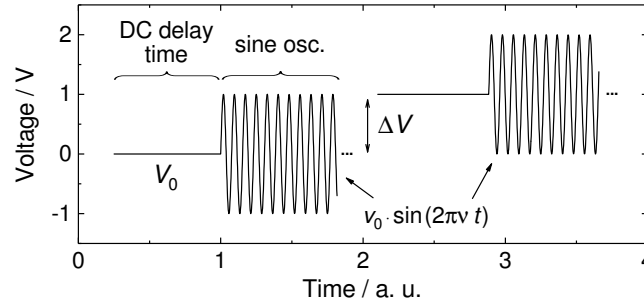


FIG. 4. Illustration of the AC modulated voltage ramp applied to the Langmuir probe.

III. EXPERIMENTAL REALIZATION AND ICP SETUP**A. AC and DC probe system**

For the realization of the AC technique the usual voltage ramp applied to the probe is modified as illustrated in Fig. 4: at each DC voltage step V_0 the sinusoidal AC signal is superimposed after a certain delay time t_{DC} , i. e.

$$V_{\text{step}}(t) = \begin{cases} V_0 & t \leq t_{DC} \\ V_0 + v_0 \sin(2\pi\nu t) & t > t_{DC} \end{cases} \quad (18)$$

With this concept, both the standard I - V characteristic and the second derivative via Eq. (5) can be obtained. The respective electronic system was developed at the Max Planck Institute for Plasma Physics in Garching (Germany) and generates the output voltage via a microcontroller and 16-bit D/A converter. Fourier analysis of the noise spectrum at the experiment used (see section III B) led to the choice of the fixed modulation frequency of 13 kHz. Freely selectable parameters are the DC delay time, the number of superimposed sine oscillations per voltage step and the number of equidistant steps of the applied voltage ramp (max. ± 75 V). Moreover, the size of the modulation amplitude can be varied up to ≈ 1.5 V. Probe currents are measured via an implemented shunt (1Ω) up to 100 mA. The AC system communicates with a controlling computer via a USB interface using a fiber optic extender to ensure galvanic isolation. The output voltage and measured current are recorded over time with a USB oscilloscope (PicoScope 5443A with maximum bandwidth of 100 MHz). For the simultaneous use of two channels the scope provides a sufficient vertical resolution of 15 bit with a memory buffer of up to 32 MSamples. It is powered only by the computer in order to avoid possible ground loops.

After the completion of one measurement the data stored in the buffer of the scope is trans-

Application of a Langmuir probe AC technique

ferred to the computer and evaluated using a LabVIEW program, which is briefly described in the following. The recorded voltage ramp is separated into its steps according to Eq. (18) and the AC part is fitted with a sinusoidal function using the Levenberg-Marquardt algorithm to retrieve the actual DC bias V_0 , the exact modulation frequency ν_{sin} and the modulation amplitude ν_0 for each step. The corresponding current steps are attributed to the output voltage over time. Here, each DC part is averaged for the construction of the conventional I - V characteristic. For the respective AC parts a fast Fourier transformation (FFT) with Hann windowing and DC filtering is applied in order to obtain the current spectra. This is done for a precisely chosen amount of samples, which is explained in detail in section IV. From the current spectra, the peak values at twice the modulation frequency $I_p^{26\text{kHz}}$ are used to calculate the EEDF via Eq. (6). The EEDF can be fitted with the so-called ν -distribution, which is a parameterized distribution of the form^{33,34}

$$\text{EEDF}^\nu(\epsilon_e) = c_\nu n_e \langle \epsilon_e \rangle^{-3/2} \sqrt{\epsilon_e} \exp \left[-b_\nu \left(\frac{\epsilon_e}{\langle \epsilon_e \rangle} \right)^\nu \right], \quad (19)$$

with

$$b_\nu = \left[\frac{\Gamma(2.5/\nu)}{\Gamma(1.5/\nu)} \right]^\nu \quad (20)$$

and the normalization constant

$$c_\nu = \frac{\nu b_\nu^{3/(2\nu)}}{\Gamma(1.5/\nu)}. \quad (21)$$

The ν -parameters one and two correspond to Maxwellian and Druyvesteyn^{35,36} distributions, respectively. Additionally, the electron density and mean electron energy are calculated by integration of the measured EEDF via

$$n_e = \int_0^\infty \text{EEDF}(\epsilon_e) d\epsilon_e \quad (22)$$

and

$$\langle \epsilon_e \rangle = \frac{1}{n_e} \int_0^\infty \text{EEDF}(\epsilon_e) \epsilon_e d\epsilon_e. \quad (23)$$

In case of a non-Maxwellian EEDF, an 'effective' electron temperature $T_e^{\text{eff}} = 2/3k_B^{-1} \langle \epsilon_e \rangle$ is defined.

The plasma potential, which is needed for the determination of the EEDF, can be found from where the second derivative crosses zero since it marks the inflection point of a Langmuir probe characteristic. In a typical AC measurement the voltage step resolution is set to 0.4 – 0.5 V for an appropriate measurement time and amount of sampled data (see section IV). Moreover, the

Application of a Langmuir probe AC technique

modulus of the second derivative is determined with Eq. (5), which means that the measured second derivative with the AC system does not cross zero and hence $I_p'' = 0$ could only be determined trustfully with a finer voltage step resolution. Therefore, the plasma potential is determined with a separate fully calibrated DC probe system by numerical differentiation of the I - V characteristic ($\Delta V = 0.05$ V) using a SG filter for smoothing. The DC probe system is equipped with the analysis software PlasmaMeterTM (version 5.3), allowing for complete automatic evaluation of the probe data (see detailed description in Ref. 37). Here, the determination of plasma parameters is based on the classical Langmuir theory assuming a Maxwellian EEDF: the electron temperature is obtained by the slope of a linear regression to the logarithmically plotted second derivative and the electron density is calculated from the probe current at the plasma potential and the determined electron temperature via

$$n_e = \sqrt{\frac{2\pi m_e}{k_B T_e} \frac{I_p(\phi_{pl})}{eA_p}}. \quad (24)$$

This straightforward approach is widely used to determine plasma parameters and is henceforth called standard evaluation procedure.

B. ICP experiment

As shown in the schematic block diagram in Fig. 5, the AC system is implemented at a well characterized ICP experiment³⁸ consisting of a cylindrical stainless steel vacuum vessel with 15 cm in diameter and 10 cm in height. A water cooled planar RF antenna with seven windings is used, which is located in an evacuated chamber on top of the vessel and separated from the plasma chamber by a 3 mm thin dielectric quartz plate. The solenoid is connected to an RF generator via a matching network, operating at 2 MHz with a maximal output power of 2 kW. The working gas (in this work argon and hydrogen) is fed to the discharge vessel via calibrated mass flow controllers and the pressure is measured via a capacitive pressure gauge. The Langmuir probe is inserted horizontally at half height of the vessel and is movable with a linear drive mechanism. As probe tip a tungsten wire is used, with a radius of $r = 25 \mu\text{m}$ and length of $l = 2$ mm in argon and $r = 150 \mu\text{m}$ and $l = 10$ mm in hydrogen (comparable probe currents in the mA range at the same operational parameters). The tungsten wire is fed in a thin quartz capillary with a diameter of only 1 mm to minimize plasma perturbations and is mounted on a cylindrical ceramic shaft. The probe is biased with respect to the grounded vessel wall and is connected to the AC system via a triaxial cable for appropriate RF shielding. Moreover, the probe is equipped with a passively working RF

Application of a Langmuir probe AC technique

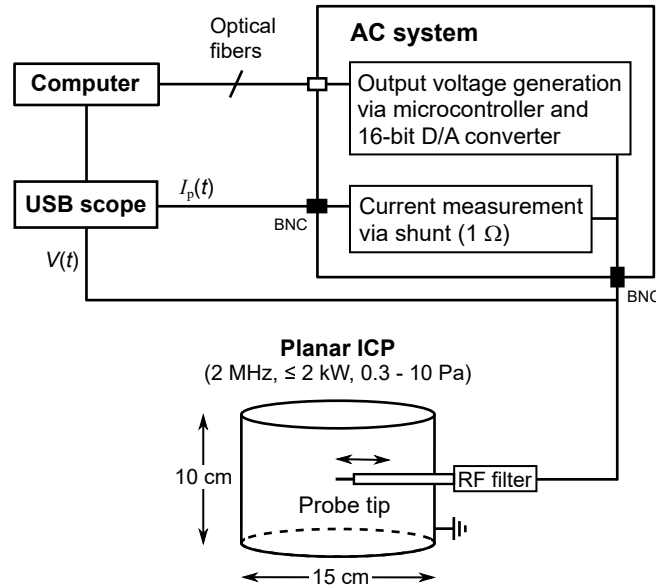


FIG. 5. Schematic block diagram of the AC system implemented at the ICP experiment used in this work.

compensation filter with a floating reference electrode placed a few millimeters behind the probe tip. A more detailed description of the Langmuir probe and the RF compensation circuit is given in Ref. 37.

The evaluation of the EEDF using the Druyvesteyn formula requires the presence of a collisionless probe sheath, which in weakly ionized plasmas corresponds to the condition³⁹

$$\lambda_e \gg d + h. \quad (25)$$

Here, λ_e denotes the electron mean free path, $d = r \ln[\pi l / (4r)]$ the characteristic cylindrical probe dimension and h the sheath thickness, which is estimated by $h \approx \lambda_D [e|V - \phi_{pl}| / (k_B T_e)]^{3/4}$ with the electron Debye length λ_D . The electron mean free path is given by $\lambda_e = (n\sigma_e)^{-1}$, where σ_e is the energy dependent effective momentum transfer cross section (cf. Ref. 40) and n the particle density of the collision partners, which as a good approximation is the neutral particle density. In this work, λ_e is usually around two orders of magnitude higher than the characteristic probe dimension plus the sheath thickness and thus inequality (25) is fulfilled. Furthermore, the large discharge volume of 1767 cm³ guarantees a fast enough replenishment of the removed electrons by the probe⁴¹. To avoid distortions by impurities on the probe surface, a high DC bias is applied regularly to thermally desorb all residuals.

Application of a Langmuir probe AC technique

IV. CHARACTERIZATION OF THE AC SYSTEM

The AC system was benchmarked by comparing its DC probe characteristic to the DC probe system at the same discharge. Both I - V characteristics agree within the reproducibility of the respective systems, which confirms the basic applicability of the AC system. Since the AC system provides a high flexibility with regard to the modulation of the output voltage, suitable modulation parameters for the determination of the second derivative are identified first.

A. Number of sine oscillations per step

In order to ensure an appropriate resolution of the recorded current-voltage data in the time domain, the sampling frequency of the applied oscilloscope is set to $v_{\text{sample}} = 200$ kHz. With this sampling rate the Nyquist limit is set to 100 kHz, which covers the first seven harmonics of the 13 kHz modulation frequency and thus guarantees proper sampling of the current signal. In Fig. 6(a) some recorded cycles of applied voltage oscillations and the corresponding probe current response are shown exemplary. Since the FFT processing gain increases with increasing number of samples, the signal-to-noise ratio (SNR) for determining the current amplitude $I_p^{26\text{kHz}}$ at twice the modulation frequency can be improved by a higher number of applied sine oscillations. This is demonstrated in Fig. 6(b), where current frequency spectra corresponding to 50 and 500 applied sine oscillations are shown around 26 kHz. The increase of the Fourier transformed samples N by a factor of 10 leads to a 10 times higher resolution in the frequency domain ($\Delta v = v_{\text{sample}}/N$) and to a reduction of the noise floor by roughly 11.5 dB. According to Eq. (5) the amplitude of the second harmonic is given by

$$I_p^{26\text{kHz}} = \frac{v_0^2}{4} I_p'' \quad (26)$$

and thus solely determined by the value of the second derivative for a fixed modulation amplitude. Since I_p'' generally decreases with an increasing voltage difference to the plasma potential, a lower noise floor consequently leads to a higher accessible dynamic range of the distribution function. Furthermore, a high resolution in the frequency spectrum allows a more precise determination of the current amplitude at exactly twice the modulation frequency, which is $2v_{\text{sin}} = 25.988$ kHz. Since the FFT noise floor reaches a minimum at around 400 oscillations taken in the time domain, the input parameter is set to 500 oscillations per voltage step in order to have a proper margin for the selection of FFT samples in the automatic LabVIEW evaluation. With this, an appropriate

Application of a Langmuir probe AC technique

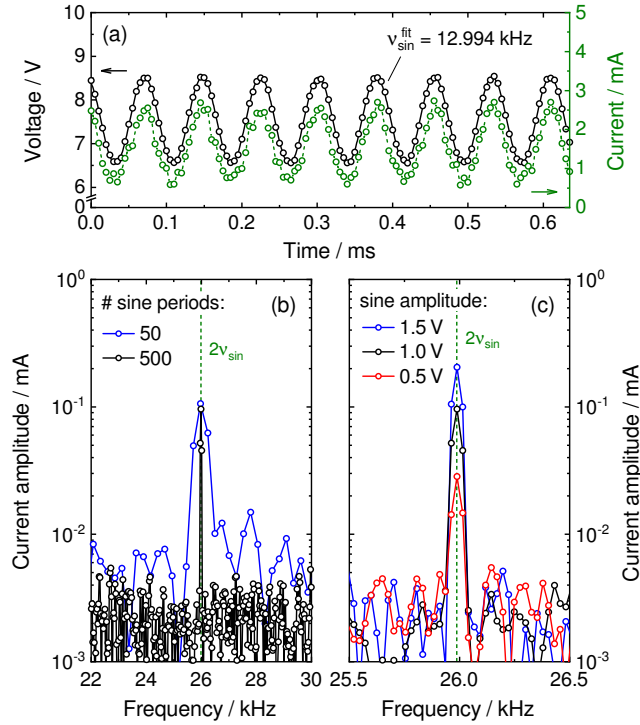


FIG. 6. (a) Recorded raw data of some applied voltage oscillations with 1.0 V amplitude and the corresponding probe current response. The voltage cycles are fitted with a sinusoidal function. (b) FFT spectra of measured AC perturbed probe currents for 50 and 500 applied voltage oscillations with amplitude 1.0 V. (c) FFT spectra for 500 applied voltage oscillations with an amplitude variation between 0.5 V and 1.5 V.

resolution of around 26 Hz is achieved in the frequency domain.

B. Sine amplitude

From relation (26) it gets clear that the SNR in the frequency domain can be improved by increasing the sine amplitude. This is demonstrated in Fig. 6(c), where the increase of the sine amplitude from 0.5 V to 1.5 V leads to an increase of the SNR by 17.2 dB. However, a higher modulation amplitude goes at the expense of accuracy since the neglected terms in Eq. (4) gain a higher weight. Moreover, the modulation amplitude determines the lower limit of the electron energy up to which the EEDF can be evaluated since the probe voltage \tilde{V} has to stay below the plasma potential. Hence, it was chosen to vary the sine amplitude from 0.5 V just below the plasma potential to 1.5 V in the higher energy region to simultaneously optimize SNR, energy resolution and accuracy. The upper limit of 1.5 V is a technical restriction of the current electronics employed

Application of a Langmuir probe AC technique

and the lower limit of 0.5 V was found to be appropriate in order to keep a reasonable SNR at the typical plasma parameters in this work. To improve the SNR for modulation amplitudes lower than 0.5 V, a more sophisticated electronic system with lock-in and bandpass amplifiers²¹ might be useful.

Table I summarizes the input parameters for the AC system used in this work. The output voltage is equidistantly ramped up from typically -10 V to 20 V with $\Delta V = 0.4$ V. With the chosen DC delay time of 5 ms, one measurement takes around 3.2 s and consists of roughly 0.65 MSamples.

C. Error estimation

For the application of the AC technique some sources of error have to be considered. Firstly, the systematic overestimation of the second derivative is dependent on the modulation amplitude and the shape of the EEDF. At the present ICP and in the investigated parameter range, the (effective) electron temperature usually lies in the range of 2 – 5 eV. Hence, a comparison with Fig. 2 shows that this error is $< 1\%$ in the low energy range where an amplitude of only 0.5 V is used and stays below 5 % in the high energy range where the amplitude is 1.5 V. Furthermore, investigation of the noise spectra at typical plasma conditions in argon and hydrogen reveals the dominant distortion frequency at 2 MHz, whose amplitude, however, stays below 0.1 V and is compensated by the implemented RF filter. Consequently, intermodulation effects can be neglected.

Secondly, the determination of the current amplitude at twice the modulation frequency via FFT processing is very sensitive to discretization, i. e. it is dependent on how good $2v_{\text{sin}}$ is resolved in the discrete current spectrum. If $2v_{\text{sin}}$ lies exactly in between two samples, the error is maximized. Therefore, the control parameter

$$\eta = \frac{2v_{\text{sin}}}{\Delta v} = \frac{2v_{\text{sin}}}{v_{\text{sample}}} N \quad (27)$$

is calculated during the automatic evaluation procedure, with N being the chosen amount of samples in the time domain comprising ≈ 400 oscillations. By assuring that the deviation of η from the next integer value is less than 10 % via fine-adjustment of N , the FFT error stays below 1 %.

TABLE I. Input parameter set for the AC system.

ΔV	t_{DC}	# osc.	v_0	v_{sin}	v_{sample}
0.4 V	5 ms	500	0.5 – 1.5 V	13 kHz	200 kHz

Application of a Langmuir probe AC technique

Since the data is recorded with an oscilloscope, the instrument function is assumed to be a sharp delta function and a deconvolution procedure is thus not performed.

To have an order-of-magnitude estimate of the displacement current, the DC probe sheath capacitance is calculated by the approximation

$$C_{\text{sh}}^{\text{DC}} = \frac{A_p}{2^{5/4}} \frac{\epsilon_0}{\lambda_D} \left[\frac{e(\phi_{\text{pl}} - V)}{k_B T_e} \right]^{-3/4} \quad (28)$$

with ϵ_0 being the permittivity of free space and $V < \phi_{\text{pl}}$ ³². For typical plasma parameters in this work this yields $C_{\text{sh}}^{\text{DC}} \lesssim 1$ pF and according to relation (17) $I_{\text{disp}} \approx C_{\text{sh}}^{\text{DC}} 2\pi v_{\text{sin}} v_0 \lesssim 10^{-7}$ A. Since the usual noise floor is more than one order of magnitude higher than this value (see Fig. 6), the measured probe current can be considered as solely particle current determined by the nonlinear sheath resistance.

Lastly, the plasma potential is determined from the zero-crossing of the two-time numerical differentiated I - V characteristic using SG smoothing. This procedure typically results in an uncertainty of ± 0.5 V.

Given all these considerations, the total error of the determined EEDF via Eq. (6) is restricted to ± 10 % for measurements in this work.

D. Proof of concept

In Fig. 7 measured EEDFs are shown both via the AC method and via numerical differentiation of the I - V characteristic (DC method) in argon at 4 Pa gas pressure and 300 W RF power close to the vessel edge. The numerical differentiation is performed by using SG smoothing with different filter parameters: in Fig. 7(a) the polynomial degree is $M = 2$ with window sizes of $n = 30$ and $n = 60$ points, and in Fig. 7(b) $M = 4$ with $n = 40$ and $n = 80$, respectively. For a better visualization, the so-called electron energy probability function (EEPF) is plotted on a semi-logarithmic scale, which is defined as $\text{EPPF} = \text{EEDF} / \sqrt{\epsilon_e}$ (linear evolution in case of a Maxwellian EEDF). In this representation, a distortion of the second derivative near the plasma potential typically manifests as an unphysical drop near zero energy⁵, leading to a lack of information about the low energy electrons.

In the mid energy range the AC and DC EEPFs agree very well, which principally verifies the AC technique. For energies below 4 eV, however, the DC EEPFs start to flatten compared to the AC EEPF. The flattening of the DC EEPFs depends on the applied SG filter parameters and ends up

Application of a Langmuir probe AC technique

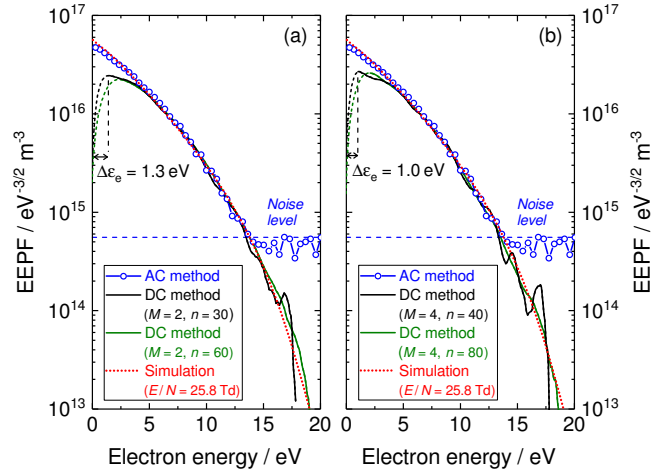


FIG. 7. EEPF measurement in argon (4 Pa, 300 W) close to the vessel edge via AC method and via DC method using SG smoothing with (a) polynomial degree $M = 2$ and window sizes of $n = 30$ and $n = 60$ points and (b) polynomial degree $M = 4$ and window sizes of $n = 40$ and $n = 80$ points. The energy gap $\Delta\epsilon_e$ in the low energy range of the DC EEPFs is depicted as dashed line for $n = 30$ and $n = 40$, respectively. A simulation of the EEPF is performed with BOLSIG+, using the cross sections recommended by Phelps^{40,42}.

in a drop in the low energy range. This depletion has no physical reason under the given conditions and is therefore depicted as dashed line. According to the requirements given by Godyak⁴³, the energy gap $\Delta\epsilon_e$ between zero and maximum of the EEPF should not exceed 20 – 30 % of the mean electron energy $\langle\epsilon_e\rangle$ in a 'good' probe measurement. For the SG filter with $M = 2$ and $n = 30$, $\Delta\epsilon_e = 1.3$ eV and measures 28 % of the mean electron energy determined by integration of the AC EEDF ($\langle\epsilon_e\rangle_{AC} = 4.6$ eV). Increasing the window size to $n = 60$ results in a higher distortion of the EEPF maximum, but in a better smoothing of the EEPF high energy tail. Higher order polynomials with $n = 40$ lead to a sharper low energy peak with $\Delta\epsilon_e = 1.0$ eV = $0.22\langle\epsilon_e\rangle_{AC}$. However, for sufficient smoothing in the high energy range larger windows are required, leading again to a flattening effect of the EEPF maximum. This confirms that the resulting DC EEPF is strongly affected by the smoothing parameters. In contrast, a depletion in the low energy range is not observed in the measured AC EEPF.

A simulation of the EEPF is performed with the freely available electron Boltzmann equation solver BOLSIG+ (version 03/2016), which is well benchmarked for argon plasmas⁴⁴. Using experimentally measured values as input parameters under consideration of electron-electron collisions, the simulation result shows an excellent agreement with the AC measurement. The corresponding

Application of a Langmuir probe AC technique

reduced electric field E/N , which is given as output parameter, is a rather low value of 25.8 Td, which is due to the measurement close to the plasma edge.

In Fig. 8 an AC measurement is shown in argon at 5 Pa gas pressure and 300 W RF power in the vessel center. Again, a depletion in the low energy range is not observed and the measurement shows an excellent agreement with the simulation performed with BOLSIG+ ($E/N = 94.9$ Td). The result obtained via numerical differentiation reveals a higher noise magnitude in the probe current which is barely visible in the I - V trace: SG smoothing with $M = 2$ and $n = 30$ in Fig. 8(a) and $M = 4$ and $n = 40$ in Fig. 8(b) lead to an oscillation in the low energy range, which is not the case for the measurement shown in Fig. 7. Suppression of this noise can be achieved with a larger SG smoothing window, which is, however, accompanied by a depleted EEPF in the low energy range ($\Delta\varepsilon_e = 0.53\langle\varepsilon_e\rangle_{AC}$ in the case of $M = 2$ and $n = 60$ and $\Delta\varepsilon_e = 0.25\langle\varepsilon_e\rangle_{AC}$ for $M = 4$ and $n = 80$).

The exemplary AC measurements in argon demonstrate a reliable access to the EEDF low energy range below 1 eV. From the comparison to numerical differentiation using SG smoothing it can be concluded that the AC technique is more efficient in the low energy region, especially in noisy environments. Numerical differentiation with SG filtering requires stabilized signals with low noise to achieve a sharp energy resolution near zero energy^{6,27}. Since low energy electrons typically constitute the majority of the ensemble, the AC system can contribute to a trustworthy evaluation of plasma parameters by integration of the EEDF.

Dependent on the applied SG filter parameters the dynamic range of the DC EEPF is typically about 1 – 2 orders of magnitude higher than accessible with the current AC system. As shown by Roh *et al.*⁸, a better smoothing in the high electron energy tail via numerical differentiation could be obtained with the use of a Blackman filter. However, at the same time this filter can lead to a more severe distortion in the low energy range than the SG filter. To increase the SNR of the AC system in the high energy regime, further noise reduction techniques or a higher modulation amplitude than 1.5 V should be applied.

V. EEDF MEASUREMENTS IN HYDROGEN

EEDF measurements in hydrogen are carried out due to the fact that a strong variation of the distribution function is given for different operational parameters with electron densities 1 – 2 orders of magnitude lower than in argon. The measurements are performed with the AC system

Application of a Langmuir probe AC technique

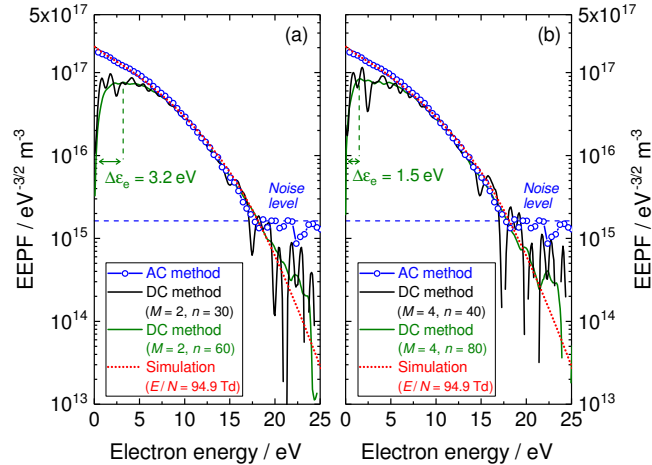


FIG. 8. Comparison of measured EEPFs in argon (5 Pa, 300 W) in the vessel center via the AC method and via numerical differentiation of a noisy I - V characteristic using SG smoothing with (a) polynomial degree $M = 2$ and window sizes of $n = 30$ and $n = 60$ points and (b) polynomial degree $M = 4$ and window sizes of $n = 40$ and $n = 80$ points. The energy gap $\Delta\epsilon_e$ of the DC EEPFs is depicted as dashed line for $n = 60$ and $n = 80$, respectively. The EEPF simulation is performed with BOLSIG+^{40,42}.

in the center of the discharge at 5 Pa and 10 Pa gas pressure and RF output powers in the range of 600 – 1000 W.

A. Evolution of the EEDFs

In Fig. 9 the measured EEPFs are plotted in absolute numbers in the upper diagrams and are normalized to the respective electron densities in the lower diagrams. At 5 Pa gas pressure the EEPFs can be determined for energies up to 20 eV. At 800 W fitting with the parameterized distribution (19) leads to a ν -parameter of 2.0, which corresponds to a Druyvesteyn distribution. By increasing the RF power up to 1000 W, the absolute EEPF is shifted upwards due to an increased electron density. Since the ν -parameter is reduced to 1.7, the increase of the RF power leads to a higher percentage of low energy electrons and therefore to an intersection point of the normalized EEPFs at around 7.5 eV. By rising the gas pressure up to 10 Pa, the EEPFs show a much steeper progression and a higher dynamic range in the accessible energy interval up to 10 – 15 eV. At 800 W the EEPF follows a ν -distribution with $\nu = 1.6$ up to approximately 8 eV and lies above the extrapolated ν -fit for higher energies. By decreasing the RF power to 600 W the concaveness of the EEPF in the semi-logarithmic representation is increased in the low energy range and up

Application of a Langmuir probe AC technique

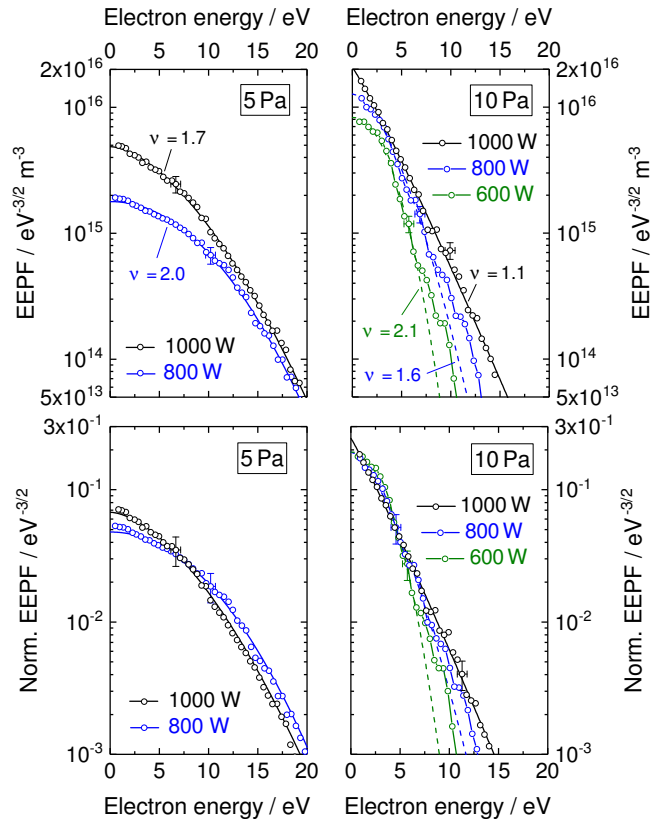


FIG. 9. EEPFs measured with the AC system in H_2 at different gas pressures and RF powers. The absolute EEPFs from the upper diagrams are normalized to the electron density in the lower diagrams. The EEPFs are fitted with ν -distributions.

to 7 eV the EEPF can be described with a $\nu = 2.1$ distribution. For higher energies the measured EEPF lies again above the extrapolated fit. At 10 Pa and 1000 W, the EEPF can be described by a ν -distribution of $\nu = 1.1$ in the whole accessible energy range up to ≈ 15 eV. This closely resembles a Maxwell distribution, probably due to increased electron-electron collisions. The normalized EEPFs at 10 Pa gas pressure have a common intersection point at around 5 eV. Contrary to the measurements at 5 Pa, the increase of RF power leads to a slightly lower percentage of electrons in the low energy range ($\epsilon_e \lesssim 5$ eV) and a higher proportion of electrons in the high energy range ($\epsilon_e \gtrsim 5$ eV).

B. Plasma parameters

The electron densities calculated from the distribution functions shown in Fig. 9 are plotted as a function of RF power in Fig. 10(a) and lie in the range of $10^{16} - 10^{17} \text{ m}^{-3}$. Generally, both

Application of a Langmuir probe AC technique

increasing the RF power and increasing the gas pressure lead to higher electron densities. At 5 Pa the increase of the RF power from 800 W to 1000 W leads to a rise of the electron density by a factor of two, which at 10 Pa is the case for an increase of the RF power from 600 W to 1000 W. At 800 W the change from 5 Pa to 10 Pa leads to an increase of the density by 89 % and at 1000 W by 26 %. The densities obtained from the AC EEDFs are compared to the standard evaluation of the respective I - V characteristics. A relatively good agreement is given within the typical AC measurement uncertainty of 18 %. However, the standard evaluation systematically underestimates the electron density. The highest underestimation of about 30 % is given at 5 Pa gas pressure and 1000 W RF power. At 10 Pa and 1000 W the densities match best and agree to within 4 % due to a closely Maxwellian EEDF.

The mean electron energies calculated from the AC EEDFs are plotted as a function of RF power in Fig. 10(b) and lie in the range of 2 – 8 eV. While at 5 Pa gas pressure the increase of the RF power from 800 W to 1000 W leads to a reduction of the mean electron energy by roughly 1 eV, at 10 Pa the increase from 600 W to 1000 W leads to a 1 eV rise. Thus, two opposite trends are given for the different gas pressures due to the different relative behaviors of the distribution functions (see lower diagrams in Fig. 9). A distinct effect is, however, given for an increasing gas pressure at constant RF power: both at 800 W and 1000 W the increase of the gas pressure by a factor of two leads to a decrease of the mean electron energy (–51 % at 800 W and –38 % at 1000 W). This can be explained by a reduced ion diffusion loss to the vessel walls due to an increased collisionality, leading to a lower ionization rate. The mean electron energies are again compared to the standard evaluation. Since at 5 Pa the EEPFs are strongly concave-shaped on the semi-logarithmic plot, a linear fit in the mid energy range leads to an overestimation of the low energy electrons and hence to an underestimation of the mean electron energy by around 20 %. At 10 Pa the deviation is much smaller due to a steeper progression of the EEPFs.

Since the respective DC EEDFs are depleted in the low energy range, integration would lead to an underestimation of the electron densities of about 15 – 30 % and an overestimation of the mean electron energies of about 0.5 – 1.0 eV compared to the AC values given in Fig. 10. An enhancement of the dynamic range of the AC EEPFs would allow an even more precise determination of the electron densities and mean electron energies, which could be done by either improving the SNR of the AC measurement or by using the high energy tail from the DC measurement. However, since the low energy electrons constitute the majority of the electron ensemble in the current work, this would improve the accuracy of the plasma parameters only by a few percent.

Application of a Langmuir probe AC technique

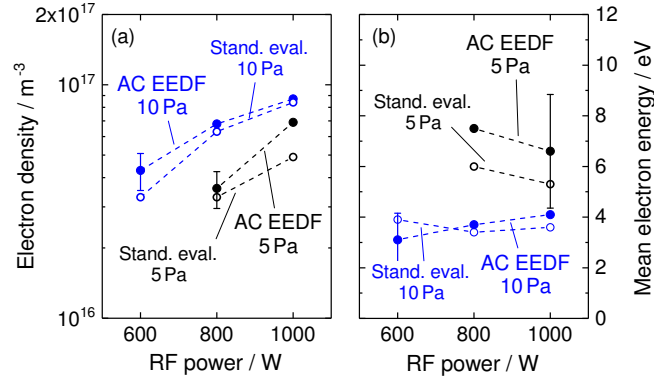


FIG. 10. Plasma parameters determined by integration of the measured electron energy distributions shown in Fig. 9 and via standard evaluation of the respective I - V characteristics: (a) Electron densities. (b) Mean electron energies.

VI. CONCLUSIONS

The well-known method of modulating the Langmuir probe bias with a small sine oscillation allows a direct measurement of the EEDF by exploitation of the second harmonic in the current response. For the application of this technique a newly developed probe system was presented in this paper. The electronic system used offers a high flexibility thanks to the usage of a microcontroller and can thus be optimized in terms of SNR, energy resolution and accuracy by a suitable interplay of sine amplitude (≤ 1.5 V), sine oscillations per voltage step and sampling frequency due to the usage of an oscilloscope. Moreover, the easy-to-use setup is equipped with an automatic data acquisition and analysis system, with which the EEDF is determined with an accuracy of $\pm 10\%$. Dedicated measurements in argon compared to a fully calibrated conventional DC probe system as well as simulations performed with the Boltzmann equation solver BOLSIG+ demonstrated applicability of the method and showed a reliable access to the low energy range of the EEDF. It was shown that the distribution functions are accurately measured down to energies below 1 eV. Furthermore, a dynamic range of about two orders of magnitude is accessible with the current maximum modulation amplitude of 1.5 V.

Since it is known that in weakly ionized low pressure plasmas the electrons are generally not in thermal equilibrium, integration of the EEDF is the preferable way to reliably obtain basic plasma parameters. The application of the AC system to hydrogen plasmas revealed a highly varying shape of the EEDF dependent on gas pressure and RF power and confirmed the non-Maxwellian nature of the plasma electrons. An evolution from Druyvesteyn to Maxwellian to distributions

Application of a Langmuir probe AC technique

which can only partially be described by a ν -distribution was observed. Therefore, the application of standard evaluation techniques with the assumption of Maxwellian electrons can lead to erroneous electron densities and mean electron energies. Furthermore, the EEDF determines electron transport or rate coefficients needed for modeling approaches. An accurate determination of the EEDF low energy range, which typically constitutes the majority of the electron ensemble, is thus indispensable for accurately studying plasma electron kinetics.

ACKNOWLEDGEMENTS

The authors thank Martin Kammerloher from Max-Planck-Institut für Plasmaphysik (Garching) for the layout and realization of the AC electronic system.

REFERENCES

- ¹M. A. Lieberman and A. J. Lichtenberg, *Principles of Plasma Discharges and Materials Processing*, 2nd ed. (Hoboken, NJ: Wiley, 2005).
- ²V. A. Godyak, R. B. Piejak, and B. M. Alexandrovich, “Probe diagnostics of non-Maxwellian plasmas,” *Journal of Applied Physics* **73**, 3657–63 (1993).
- ³M. J. Druyvesteyn, “Der Niedervoltbogen,” *Zeitschrift für Physik* **64**, 781–98 (1930).
- ⁴Y. M. Kagan and V. I. Perel’, “PROBE METHODS IN PLASMA RESEARCH,” *Soviet Physics Uspekhi* **6**, 767–93 (1964).
- ⁵V. A. Godyak and V. I. Demidov, “Probe measurements of electron-energy distributions in plasmas: what can we measure and how can we achieve reliable results?” *Journal of Physics D: Applied Physics* **44**, 233001 (2011).
- ⁶F. Magnus and J. T. Gudmundsson, “Digital smoothing of the Langmuir probe $I - V$ characteristic,” *Review of Scientific Instruments* **79**, 073503 (2008).
- ⁷J. L. Jauberteau and I. Jauberteau, “Determination of the electron energy distribution function in the plasma by means of numerical simulations of multiple harmonic components on a Langmuir probe characteristic—measurements in expanding microwave plasma,” *Measurement Science and Technology* **18**, 1235–1249 (2007).
- ⁸H.-J. Roh, N.-K. Kim, S. Ryu, S. Park, S.-H. Lee, S.-R. Huh, and G.-H. Kim, “Determination of electron energy probability function in low-temperature plasmas from current – Voltage charac-

Application of a Langmuir probe AC technique

- teristics of two Langmuir probes filtered by Savitzky–Golay and Blackman window methods,” *Current Applied Physics* **15**, 1173–83 (2015).
- ⁹J. I. Fernández Palop, J. Ballesteros, V. Colomer, and M. A. Hernández, “A new smoothing method for obtaining the electron energy distribution function in plasmas by the numerical differentiation of the I - V probe characteristic,” *Review of Scientific Instruments* **66**, 4625–36 (1995).
- ¹⁰I. D. Sudit and F. F. Chen, “RF compensated probes for high-density discharges,” *Plasma Sources Science and Technology* **3**, 162–8 (1994).
- ¹¹V. A. Godyak, R. B. Piejak, and B. M. Alexandrovich, “Measurement of electron energy distribution in low-pressure RF discharges,” *Plasma Sources Science and Technology* **1**, 36–58 (1992).
- ¹²U. Flender, B. H. Nguyen Thi, K. Wiesemann, N. A. Khromov, and N. B. Kolokolov, “RF harmonic suppression in Langmuir probe measurements in RF discharges,” *Plasma Sources Science and Technology* **5**, 61–69 (1996).
- ¹³A. Dyson, P. Bryant, and J. E. Allen, “Multiple harmonic compensation of Langmuir probes in rf discharges,” *Measurement Science and Technology* **11**, 554–559 (2000).
- ¹⁴E. Alexeff and D. F. Howell, “Simple Circuit for Obtaining the Electron Energy Distribution in a Plasma,” *Journal of Applied Physics* **40**, 4877–82 (1969).
- ¹⁵K. F. Schoenberg, “Pulsed electrostatic probes as a diagnostic for transient plasmas,” *Review of Scientific Instruments* **49**, 1377–83 (1978).
- ¹⁶K. Takahashi, C. Charles, R. Boswell, W. Cox, and R. Hatakeyama, “Transport of energetic electrons in a magnetically expanding helicon double layer plasma,” *Applied Physics Letters* **94**, 191503 (2009).
- ¹⁷R. L. F. Boyd and N. D. Twiddy, “Electron energy distributions in plasmas. I,” *Proceedings of the Royal Society of London. Series A. Mathematical and Physical Sciences* **250**, 53–69 (1959).
- ¹⁸G. R. Branner, E. M. Friar, and G. Medicus, “Automatic Plotting Device for the Second Derivative of Langmuir Probe Curves,” *Review of Scientific Instruments* **34**, 231–7 (1963).
- ¹⁹H. Amemiya and K. Shimizu, “Frequency dependence of the alternating current method for measuring the electron energy distribution function in plasmas,” *Journal of Physics E: Scientific Instruments* **12**, 581–83 (1979).
- ²⁰K. F. Schoenberg, “Electron distribution function measurement by harmonically driven electrostatic probes,” *Review of Scientific Instruments* **51**, 1159–62 (1980).

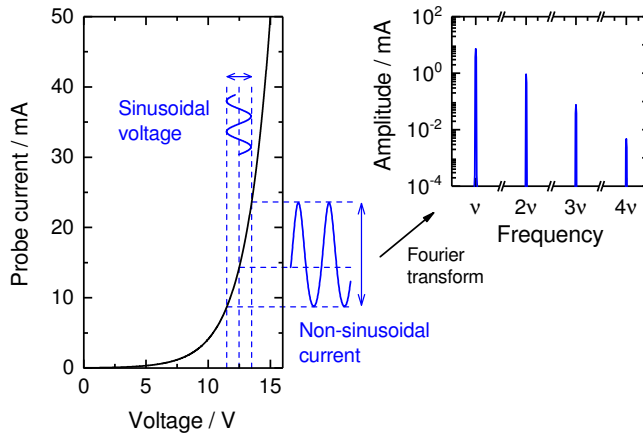
Application of a Langmuir probe AC technique

- ²¹U. Kortshagen and H. Schlüter, “Determination of electron energy distribution functions in surface wave produced plasmas. II. Measurements,” *Journal of Physics D: Applied Physics* **24**, 1585–1593 (1991).
- ²²Z. C. Lu, J. E. Foster, T. G. Snodgrass, J. H. Booske, and A. E. Wendt, “Measurement of electron energy distribution function in an argon/copper plasma for ionized physical vapor deposition,” *Journal of Vacuum Science & Technology A* **17**, 840–4 (1999).
- ²³S.-H. Seo, C.-W. Chung, J.-I. Hong, and H.-Y. Chang, “Nonlocal electron kinetics in a planar inductive helium discharge,” *Physical Review E* **62**, 7155–67 (2000).
- ²⁴B. Crowley and S. Dietrich, “A Langmuir probe system incorporating the Boyd–Twiddy method for EEDF measurement applied to an inductively coupled plasma source,” *Plasma Sources Science and Technology* **18**, 014010 (2008).
- ²⁵J. Y. Bang, A. Kim, and C. W. Chung, “Improved measurement method for electron energy distribution functions with high accuracy and reliability,” *Physics of Plasmas* **17**, 064502 (2010).
- ²⁶F. Jauberteau and J. L. Jauberteau, “Numerical differentiation with noisy signal,” *Applied Mathematics and Computation* **215**, 2283–97 (2009).
- ²⁷J.-Y. Bang and C.-W. Chung, “A numerical method for determining highly precise electron energy distribution functions from Langmuir probe characteristics,” *Physics of Plasmas* **17**, 123506 (2010).
- ²⁸R. H. Sloane and E. I. R. MacGregor, “XV. An alternating current method for collector analysis of discharge-tubes,” *The London, Edinburgh, and Dublin Philosophical Magazine and Journal of Science* **18**, 193–207 (1934).
- ²⁹W. H. Press and S. A. Teukolsky, “Savitzky-Golay Smoothing Filters,” *Computers in Physics* **4**, 669–672 (1990).
- ³⁰H. M. Mott-Smith and I. Langmuir, “The Theory of Collectors in Gaseous Discharges,” *Physical Review* **28**, 727–63 (1926).
- ³¹R. Van Nieuwenhove and G. Van Oost, “Novel Langmuir probe technique for the real-time measurement of the electron temperature,” *Review of Scientific Instruments* **59**, 1053–6 (1988).
- ³²F. F. Chen, “Time-varying impedance of the sheath on a probe in an RF plasma,” *Plasma Sources Science and Technology* **15**, 773–782 (2006).
- ³³H. W. Rundle, D. R. Clark, and J. M. Deckers, “Electron Energy Distribution Functions in an O₂ Glow Discharge,” *Canadian Journal of Physics* **51**, 144–8 (1973).

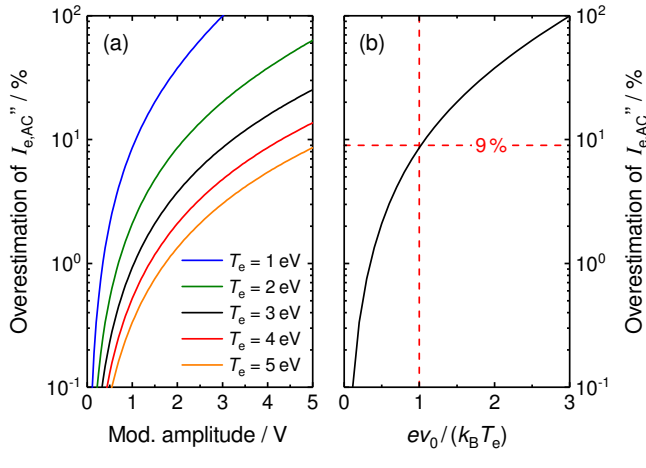
Application of a Langmuir probe AC technique

- ³⁴K. Behringer and U. Fantz, “Spectroscopic diagnostics of glow discharge plasmas with non-Maxwellian electron energy distributions,” *Journal of Physics D: Applied Physics* **27**, 2128–35 (1994).
- ³⁵M. J. Druyvesteyn and F. M. Penning, “The Mechanism of Electrical Discharges in Gases of Low Pressure,” *Reviews of Modern Physics* **12**, 87–174 (1940).
- ³⁶M. J. Druyvesteyn and F. M. Penning, “Errata: Mechanism of Electrical Discharges in Gases of Low Pressure,” *Reviews of Modern Physics* **13**, 72–3 (1941).
- ³⁷P. McNeely, S. V. Dudin, S. Christ-Koch, U. Fantz, and the NNBI Team, “A Langmuir probe system for high power RF-driven negative ion sources on high potential,” *Plasma Sources Science and Technology* **18**, 014011 (2009).
- ³⁸S. Briefi, P. Gutmann, and U. Fantz, “Alternative RF coupling configurations for H⁻ ion sources,” *AIP Conference Proceedings* **1655**, 040003 (2015).
- ³⁹V. I. Demidov, S. V. Ratynskaia, and K. Rypdal, “Electric probes for plasmas: The link between theory and instrument,” *Review of Scientific Instruments* **73**, 3409–39 (2002).
- ⁴⁰“Phelps database, www.lxcat.net,” Retrieved on June 29, 2019.
- ⁴¹J. F. Waymouth, “Perturbation of Electron Energy Distribution by a Probe,” *Journal of Applied Physics* **37**, 4492–7 (1966).
- ⁴²C. Yamabe, S. J. Buckman, and A. V. Phelps, “Measurement of free-free emission from low-energy-electron collisions with Ar,” *Physical Review A* **27**, 1345–52 (1983, Revised Oct 1997).
- ⁴³V. A. Godyak, “Measuring EEDF in Gas Discharge Plasmas,” in *Plasma-Surface Interactions and Processing of Materials*, edited by O. Auciello, A. Gras-Marti, J. A. Valles-Abarca, and D. L. Flamm (Springer Netherlands, Dordrecht, 1990) pp. 95–134.
- ⁴⁴G. J. M. Hagelaar and L. C. Pitchford, “Solving the Boltzmann equation to obtain electron transport coefficients and rate coefficients for fluid models,” *Plasma Sources Science and Technology* **14**, 722–33 (2005).

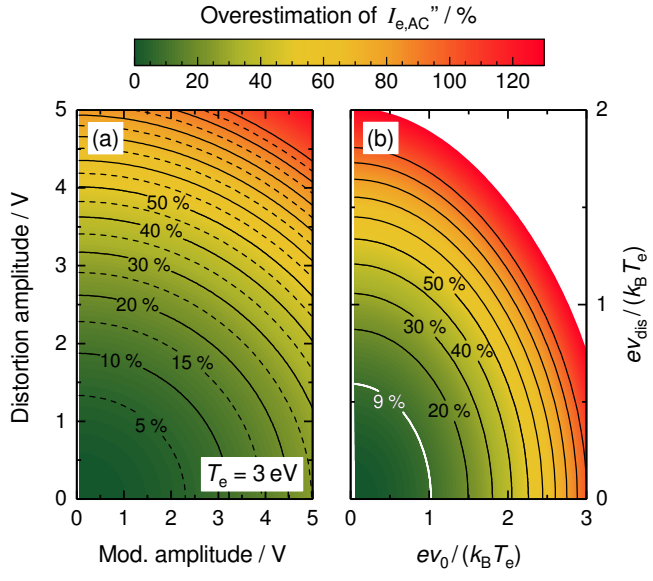
This is the author's peer reviewed, accepted manuscript. However, the online version of record will be different from this version once it has been copyedited and typeset.
PLEASE CITE THIS ARTICLE AS DOI: 10.1063/1.5139601



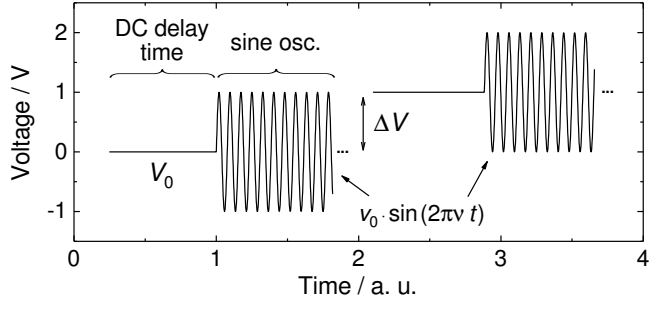
This is the author's peer reviewed, accepted manuscript. However, the online version of record will be different from this version once it has been copyedited and typeset.
PLEASE CITE THIS ARTICLE AS DOI: 10.1063/1.5139601



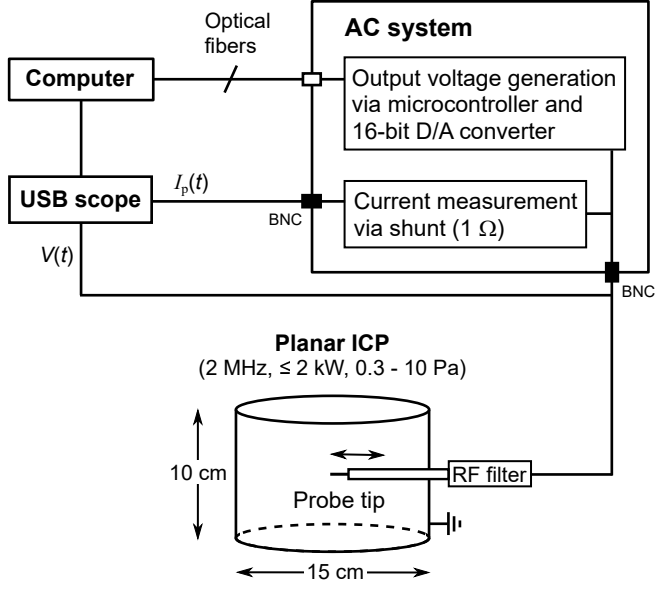
This is the author's peer reviewed, accepted manuscript. However, the online version of record will be different from this version once it has been copyedited and typeset.
PLEASE CITE THIS ARTICLE AS DOI: 10.1063/1.5139601



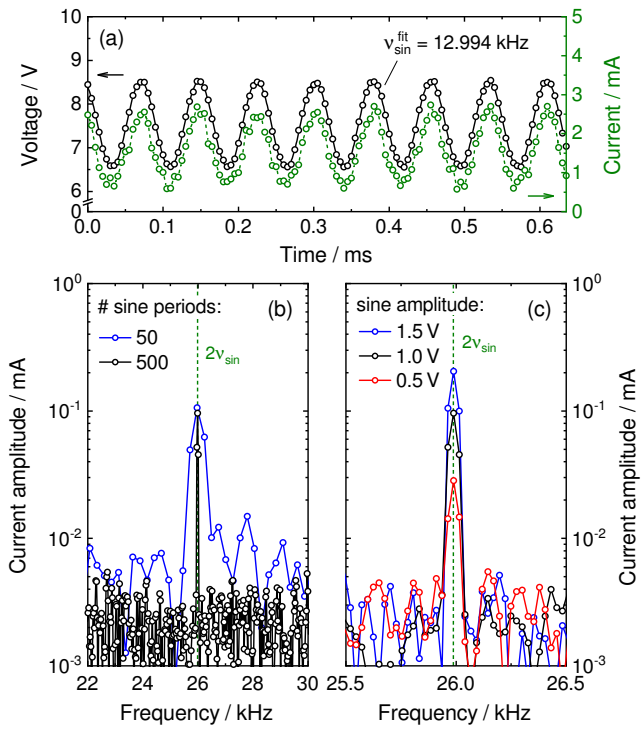
This is the author's peer reviewed, accepted manuscript. However, the online version of record will be different from this version once it has been copyedited and typeset.
PLEASE CITE THIS ARTICLE AS DOI: 10.1063/1.5139601



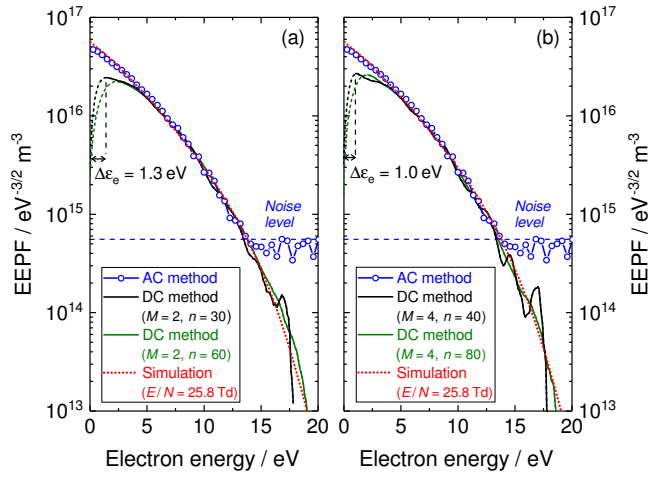
This is the author's peer reviewed, accepted manuscript. However, the online version of record will be different from this version once it has been copyedited and typeset.
PLEASE CITE THIS ARTICLE AS DOI: 10.1063/1.5139601



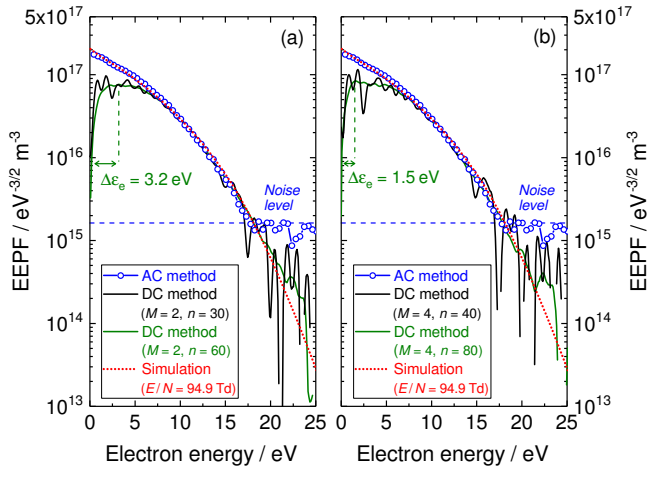
This is the author's peer reviewed, accepted manuscript. However, the online version of record will be different from this version once it has been copyedited and typeset.
PLEASE CITE THIS ARTICLE AS DOI: 10.1063/1.5139601



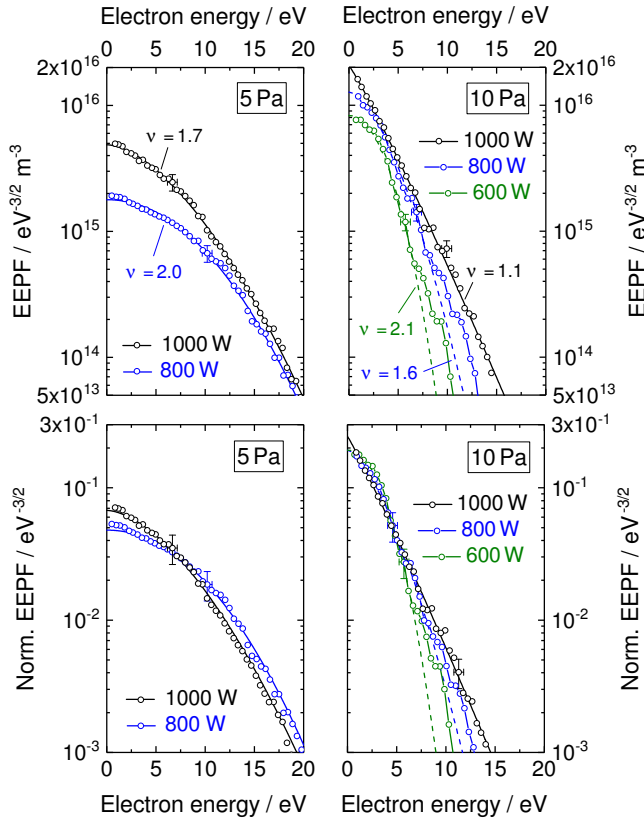
This is the author's peer reviewed, accepted manuscript. However, the online version of record will be different from this version once it has been copyedited and typeset.
PLEASE CITE THIS ARTICLE AS DOI: 10.1063/1.5139601



This is the author's peer reviewed, accepted manuscript. However, the online version of record will be different from this version once it has been copyedited and typeset.
PLEASE CITE THIS ARTICLE AS DOI: 10.1063/1.5139601



This is the author's peer reviewed, accepted manuscript. However, the online version of record will be different from this version once it has been copyedited and typeset.
PLEASE CITE THIS ARTICLE AS DOI: 10.1063/1.5139601



This is the author's peer reviewed, accepted manuscript. However, the online version of record will be different from this version once it has been copyedited and typeset.
PLEASE CITE THIS ARTICLE AS DOI: 10.1063/1.5139601

